



On oscillatory rotating convection of a couple-stress fluid with chemical reaction

Jangalla Nagaraju ^a, Kasba Ramesh Babu ^b, Gundlapally Shiva Kumar Reddy ^c,
 Kiran Kumar Paidipati ^d, and Christophe Chesneau ^{e,*}

a. *Department of Mathematics, University College of Science, Osmania University, Telangana, India, 500007.*

b. *Department of Mathematics, University College of Engineering, Osmania University, Telangana, India, 500007.*

c. *Department of Applied Sciences, National Institute of Technology Goa, Goa, India, 403401.*

d. *Area of Decision Sciences, Indian Institute of Management, Sirmaur, India.*

e. *Department of Mathematics, LMNO, CNRS-Université de Caen-Normandie, Campus II, Science 3, 14032 Caen Cedex, France.*

Received 19 June 2022; received in revised form 21 August 2023; accepted 24 December 2023

KEYWORDS

Couple-stress fluid;
 Chemical reaction;
 Linear stability
 analysis.

Abstract. Newtonian fluids fail to accurately model fluid flow behavior in various physical scenarios due to their non-Newtonian nature. This article delves into an analytical investigation of how chemical reactions impact the onset of rotating convection in a Couple-Stress (CS) fluid. Utilizing linear stability theory, we derive equations for both stationary and oscillatory Rayleigh numbers. Graphical representations illustrate the influence of key parameters such as the C_S fluid parameter, solutal Rayleigh number, Damkohler number, Lewis number, and Prandtl number on the onset of convection. The Lewis and Taylor numbers act to stabilize the system, with the Damkohler number exerting differing effects on oscillatory and stationary convection. Stationary instability is reached when the Taylor number is below 910.331, with oscillatory convection prevailing otherwise. If the Damkohler number is less than 1.76455, oscillatory instability occurs, while stationary convection dominates otherwise.

1. Introduction

Thermal instability in Newtonian fluids garners significant attention, especially in addressing geological and industrial challenges. However, when dealing with non-Newtonian fluids, which are frequently encountered in various physical scenarios, Newtonian models fall short. Among non-Newtonian fluids, Couple-Stress (CS) fluids stand out and find applications in fields like lubrication, pharmaceutical manufacturing, and

medical science [1–14]. Stokes [15] pioneered the study of C_S fluids, delving into their behavioral intricacies. This theoretical framework offers insights into the rheological characteristics of diverse complex fluids [16–19].

Hsu et al. [20] delved into the influence of C_S and surface roughness on non-Newtonian fluids. Sunil and colleagues [21] provided comprehensive global non-linear stability findings for C_S fluids. Shivakumara et al. explored the linear and weakly nonlinear stability of C_S fluids in their work [22,23]. Gaikwad and Kouser [24] delved into the thermal instability of C_S fluids in a porous layer with an internal heat source.

*. *Corresponding author.*

E-mail address: christophe.chesneau@unicaen.fr (Ch. Chesneau)

To cite this article:

J. Nagaraju, K. Ramesh Babu, G. Shiva Kumar Reddy, K. Kumar Paidipati and Ch. Chesneau “On oscillatory rotating convection of a couple-stress fluid with chemical reaction”, *Scientia Iranica* (2025), **32**(2): 6219 <https://doi.org/10.24200/sci.2023.60639.6912>

Additionally, Shivakumara and Naveen Kumar [25] examined triple diffusive convection in C_S fluids, employing a Fourier series approach to investigate weakly nonlinear theory.

Srivastava and Bera [26] studied the onset of convection in a C_S fluid within an anisotropic porous layer with a chemical reaction. Meanwhile, Malashetty and Biradar [27] explored the onset of double reaction-convection in an anisotropic porous layer. Ravi et al. [28] delved into the impact of cross diffusion on secondary convective instabilities in C_S fluids. Wolkind and Frisch [29,30] conducted the pioneering study on convection onset with reactive effects in a fluid layer. Their research considered convection in a horizontal layer of dissociating fluid. Subsequently, Bdzil and Frisch [31] delved into the thermal instability of variable density under the influence of gravitational forces in a fluid layer, examining chemical reactions in both equilibrium and non-equilibrium states within the quiescent phase. Steinberg and Brand [32,33] were the first to explore thermoconvective instabilities in a binary mixture within a reactive porous medium. Meanwhile, Gatica et al. [34] employed a variational approach to investigate oscillatory and monotonic instabilities within a porous layer, considering the impact of chemical reactions. Pritchard and Richardson [35] examined thermosolutal convection in a binary fluid confined within a porous layer. Their study assumed fixed temperatures and chemical equilibrium at the bounding surfaces, accounting for solubility variations with temperature. Using a linear stability analysis, these authors probed how solute precipitation or dissolution influenced the onset of convection. The Galerkin method was subsequently employed to advance this analysis and predict the initial bifurcation's structure.

On one hand, in their work cited as [36], Wang and Tan explored both stationary and oscillatory convection of thermosolutal instability in a porous medium with a reaction term. They focused on the Darcy-Brinkman model for a loosely packed, porous medium and investigated the relationship between the Lewis number, Darcy number, and the reaction term concerning the onset of double-diffusive convection. Additionally, in the presence of a first-order chemical reaction, Hill and Morad examined convective instabilities in an anisotropic porous medium, as documented in [37]. Their findings indicated that altering the balance between horizontal and vertical solutal diffusivities minimally affected the instability's behavior. In [38], Ward et al. conducted a comprehensive analysis of the onset of convection in an isotropic porous medium with a first-order chemical reaction. They employed stability analyses, time-dependent simulations, spectral and asymptotic methods, and stability analysis to explore this phenomenon. The authors also delved into the numerous bifurcations that emerge in

steady-state solutions. Expanding upon the work of Pritchard and Richardson [35], Sulaimi [39] extended the analysis by employing the energy method to investigate the nonlinear energy stability of the Darcy convection model with a reaction. A recent energy analysis of nonlinear convection in an anisotropic reactive porous medium was undertaken by Gautam and Narayana [40]. Their work demonstrated that altering the ratio of vertical to horizontal permeabilities had minimal impact on the instability's behavior when the solutal horizontal diffusivity exceeded the vertical diffusivity. Furthermore, in [41], Reddy and Ragoju harnessed a chemical reaction to examine the onset of instability in a Maxwell fluid-saturated porous layer. They employed analytical and numerical techniques to assess the system's stability, resolving eigenvalue problems as part of their analysis. Most recently, in [42], Reddy and colleagues examined dissolution-driven convection in a porous medium influenced by the vertical axis of rotation and a magnetic field. They employed artificial neural network modeling to predict the critical Rayleigh number, subsequently comparing these predictions to simulation results.

Moreover, traditional studies of thermal convection in confined spaces typically involve the upward flow of a fluid heated from below, a phenomenon commonly known as Rayleigh-Benard convection. This natural process plays a crucial role in various contexts, including the Earth's magnetic field reversals [43–45], where rotating convection becomes a significant and influential factor. Rotation frequently exerts its influence on fluid dynamics, affecting geophysical flows, technological processes, and astrophysical phenomena [46], including the Earth's atmosphere [47] and oceans [48–51].

The existing literature notably lacks an exploration of the impact of chemical reactions on rotating convection within a C_S fluid. This paper addresses this research gap by investigating the linear stability theory of C_S fluid in a horizontal layer featuring the Coriolis effect and chemical reactions. Our primary focus is on discerning the presence of instability and evaluating the effects of various physical parameters on linear instability.

The paper is organized as follows: Section 2 provides a comprehensive mathematical formulation. Section 3 delves into the intricacies of linear stability analysis. Section 4 showcases the key findings elucidated in this article, along with detailed discussions. Lastly, Section 5 offers the conclusion of our study.

2. Mathematical basis

We commence by establishing the mathematical framework for the problem under consideration. Our focus is on a horizontal layer of C_S fluid, which is confined

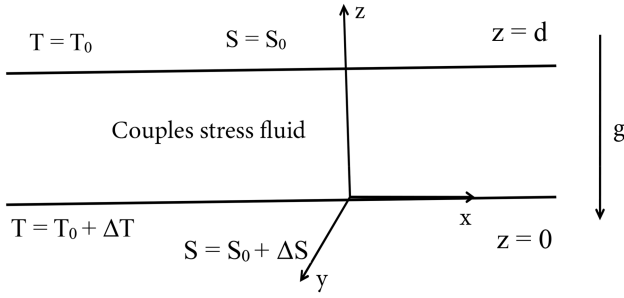


Figure 1. Physical configuration of the problem.

within the region $z \in (0, d)$. This layer maintains a constant temperature of T_0 at the upper boundary and $T_0 + \Delta T$ ($\Delta T > 0$) at the lower boundary. Additionally, the layer exhibits solute concentration levels of S_0 at the upper boundary and $S_0 + \Delta S$ ($\Delta S > 0$) at the lower boundary, as illustrated in Figure 1.

The dimensional governing equations for this system can be precisely formulated, as documented in [23,25,28,41,49].

$$\nabla \cdot \mathbf{V} = 0, \quad (1)$$

$$\rho_0 \frac{\partial \mathbf{V}}{\partial t} = -\nabla P + \mu \nabla^2 \mathbf{V} - \mu_1 \nabla^4 \mathbf{V} + \rho \mathbf{g} + 2\rho_0 \Omega (\mathbf{V} \times \hat{e}_z), \quad (2)$$

$$\frac{\partial T}{\partial t} + (\mathbf{V} \cdot \nabla) T = \kappa \nabla^2 T, \quad (3)$$

$$\frac{\partial S}{\partial t} + (\mathbf{V} \cdot \nabla) S = D_v \nabla^2 S + \chi (S_{eq}(T) - S), \quad (4)$$

$$\rho = \rho_0 (1 - \beta_T (T - T_0) + \beta_S (S - S_0)). \quad (5)$$

Assuming the equilibrium solute concentration as a linear function of the temperature, i.e., $S_{eq}(T) = S_0 + \pi(T - T_0)$, and considering chemical equilibrium at the boundaries, we can obtain $\phi = \frac{\Delta S}{\delta T}$. The conduction state is marked by:

$$T_b = \left(1 - \frac{z}{d}\right) \Delta T + T_0, \quad (6)$$

$$S_b = \left(1 - \frac{z}{d}\right) \Delta S + S_0. \quad (7)$$

In the fundamental state, we overlay minor perturbations in the following manner:

$$\begin{aligned} \mathbf{V} &= \mathbf{V}_b + \mathbf{V}', \\ T &= T_b(z) + T', \\ S &= S_b(z) + S', \\ P &= P_b(z) + P', \\ \rho &= \rho_b(z) + \rho'(x, y, z, t). \end{aligned} \quad (8)$$

To delve deeper, let us introduce the following (non-dimensional) parameters:

$$\begin{cases} (x', y', z') = d(x^*, y^*, z^*), \\ \mathbf{V}' = \frac{\kappa}{d} \mathbf{V}^*, \\ t' = \frac{d^2}{\kappa} t^*, \\ T' = (\Delta T) T^*, \\ S' = (\Delta S) S^*, \\ P' = \frac{\rho_0 \kappa^2}{d^2} P^*. \end{cases}$$

We obtain the subsequent non-dimensional equations (upon removing the asterisks):

$$\nabla \cdot \mathbf{V} = 0, \quad (9)$$

$$\frac{1}{Pr} \frac{\partial \mathbf{V}}{\partial t} = -\frac{\nabla P}{Pr} + \nabla^2 \mathbf{V} - C_S \nabla^4 \mathbf{V} + (R_T \theta - R_S S) \hat{e}_z + Ta (\mathbf{V} \times \hat{e}_z), \quad (10)$$

$$\frac{\partial \theta}{\partial t} + (\mathbf{V} \cdot \nabla) \theta = \omega + \nabla^2 \theta, \quad (11)$$

$$\frac{\partial S}{\partial t} + (\mathbf{V} \cdot \nabla) S = \omega + \frac{1}{Le} \nabla^2 S + D_v (\theta - S), \quad (12)$$

where:

$$R_T = \frac{\beta_T g \Delta T d^3}{\kappa \nu}, \quad R_S = \frac{\beta_S \Delta S d^3}{\kappa \nu}, \quad C_S = \frac{\mu_1}{\mu d^2},$$

$$Pr = \frac{\mu}{\rho_0 \kappa}, \quad Le = \frac{\kappa}{D_v}, \quad Ta = \frac{2\rho_0 \Omega d^2}{\mu}, \quad Dm = \frac{d^2 \chi}{\kappa}.$$

It is important to note that all of the terms used in the aforementioned equations have definitions in the nomenclature.

3. Linear stability analysis

3.1. Equations

Let us re-consider Eqs. (9)-(12) as:

$$\begin{aligned} \frac{1}{Pr} \frac{\partial \mathbf{V}}{\partial t} &= -\frac{\nabla P}{Pr} + \nabla^2 \mathbf{V} - C_S \nabla^4 \mathbf{V} \\ &+ (R_T \theta - R_S S) \hat{e}_z + Ta^{1/2} (\mathbf{V} \times \hat{e}_z), \end{aligned} \quad (13)$$

$$\frac{\partial \theta}{\partial t} = \omega + \nabla^2 \theta, \quad (14)$$

$$\frac{\partial S}{\partial t} = \omega + \frac{1}{Le} \nabla^2 S + Dm (\theta - S). \quad (15)$$

By extracting the third components of the curl from Eq. (13), we attain

$$\left(\frac{1}{Pr} \frac{\partial}{\partial t} - \nabla^2 + C_S \nabla^4 \right) \omega_z - Ta^{1/2} \frac{\partial w}{\partial z} = 0, \quad (16)$$

$$\left(\frac{1}{Pr} \frac{\partial}{\partial t} - \nabla^2 + C_S \nabla^4 \right) \nabla^2 w - (R_T \nabla_h^2 \theta - R_S \nabla_h^2 S) + Ta^{1/2} \frac{\partial \omega_z}{\partial z} = 0, \quad (17)$$

where ω_z represents the z -component of vorticity $((\nabla \times \mathbf{V}) \cdot \hat{e}_z)$, while w corresponds to the z -component of velocity, and

$$\nabla_h^2 = \frac{\partial^2}{\partial x^2} + \frac{\partial^2}{\partial y^2},$$

is the horizontal Laplacian operator. By removing ω_z from Eqs. (16) and (17), one obtains:

$$\left(\frac{1}{Pr} \frac{\partial}{\partial t} - \nabla^2 + C_S \nabla^4 \right)^2 \nabla^2 w - \left(\frac{1}{Pr} \frac{\partial}{\partial t} - \nabla^2 + C_S \nabla^4 \right) (R_T \nabla_h^2 \theta - R_S \nabla_h^2 S) + Ta \frac{\partial^2 w}{\partial z^2} = 0. \quad (18)$$

Introducing normal modes involves expressing perturbations in the following form:

$$(w, \theta, S) = (W(z), \theta(z), S(z)) e^{i(lx + my) + \sigma t}, \quad (19)$$

where l and m are the wave numbers along the x and y directions, respectively, with $q = \sqrt{l^2 + m^2}$ and σ is a complex parameter. Substituting the above expressions into Eqs. (14), (15), and (18), we obtain:

$$A_1^2 (D^2 - q^2) W - A_1 (R_S S - R_T \theta) q^2 + Ta D^2 W = 0, \quad (20)$$

$$\sigma \theta = W + (D^2 - q^2) \theta, \quad (21)$$

$$\sigma S = W + \frac{1}{Le} (D^2 - q^2) S + Dm (\theta - S), \quad (22)$$

$$W = \theta = S = 0 \text{ at } z = 0, 1, \quad (23)$$

where $A_1 = \left(\frac{\sigma}{Pr} - (D^2 - q^2) + C_S (D^2 - q^2)^2 \right)$, $D = \frac{d}{dz}$ and $q^2 = l^2 + m^2$. We assume that the solutions to W, θ , and S are under the following form:

$$\begin{pmatrix} W(z) \\ \theta(z) \\ S(z) \end{pmatrix} = \begin{pmatrix} W_0 \sin(\pi z) \\ \theta_0 \sin(\pi z) \\ S_0 \sin(\pi z) \end{pmatrix}, \quad (24)$$

which satisfy the boundary conditions in Eq. (23). On substituting Eq. (24) into Eqs. (20)-(22), one obtains:

$$\begin{pmatrix} A_2^2 (-\delta^2) - Ta \pi^2 & A_2 R_T q^2 & -A_2 R_S q^2 \\ 1 & (-\delta^2 - \sigma) & 0 \\ 1 & Dm & (-\frac{1}{Le} \delta^2 - Dm - \sigma) \end{pmatrix} \begin{pmatrix} W \\ \theta \\ S \end{pmatrix} = \begin{pmatrix} 0 \\ 0 \\ 0 \end{pmatrix}, \quad (25)$$

where $A_2 = \left(\frac{\sigma}{Pr} + \delta^2 + C_S \delta^4 \right)$, $\delta^2 = \pi^2 + q^2$. For the nontrivial solution of the above matrix Eq. (25), the determinant of above matrix is zero, from which one obtains the following approximate instability threshold:

$$R_{T_c} = \frac{(i\omega + \delta^2)(\pi^2 Pr^2 Ta + \delta^2 A_3^2)}{Pr q^2 A_3} + \frac{Le R_S (Dm + i\omega + \delta^2)}{Dm Le + iLe\omega + \delta^2}, \quad (26)$$

being:

$$A_3 = i\omega + Pr \delta^2 + C_S Pr \delta^4. \quad (27)$$

3.2. Stationary convection

Substituting $\omega = 0$ allows us to ascertain the critical Rayleigh number for the initiation of stationary convection (denoted as $R_{T_c}^{sc}$). This results in:

$$R_{T_c}^{sc} = \frac{\pi^2 Ta + \delta^6 (1 + C_S \delta^2)^2}{q^2 (1 + C_S \delta^2)} + \frac{Le R_S (Dm + \delta^2)}{Dm Le + \delta^2}. \quad (28)$$

For Newtonian fluid, in the absence of the Coriolis effect and chemical reaction, the above Rayleigh number reduces to:

$$R_{T_c}^{sc} = \frac{\delta^6}{q^2}, \quad (29)$$

which is well agree with the results obtained by Chandrasekhar [52].

3.3. Oscillatory convection

Now, let us delve into the examination of the real and imaginary components of R , with a requirement for the imaginary part of R to be nullified. When we substitute ω^2 into the real part of R , we arrive at the thermal Rayleigh number, denoted as $R_{T_c}^{2c}$, signifying oscillatory convection.

4. Discussion

In this article, we examine the eigenvalue problem related to the stability of thermosolutal convection in a C_S fluid and the impact of Coriolis and chemical reactions. We highlight some features of the sets of expansion functions that can be used for an analytical analysis of this problem using the spectral methods that we applied.

The behavior of the thermal critical Rayleigh number at the onset of stationary convection ($R_{T_c}^{sc}$) versus the Dm with different values of $Le = 2, 4, 6$ is displayed in Figure 2, with the other parameters held constant at $R_S = 800$, $C_S = 0.04$ and $Ta = 50$. This figure makes it clear that the Damkohler number has a destabilizing effect on a fluid layer because the Dm increases as $R_{T_c}^{sc}$ decreases.

Figure 3 illustrates the relationship between $R_{T_c}^{sc}$ and Le for various values of C_S , while keeping other parameters constant. This figure highlights the positive correlation between the values of $R_{T_c}^{sc}$ and C_S as Le increases. Consequently, it can be inferred that increasing the value of Le stabilizes the system.

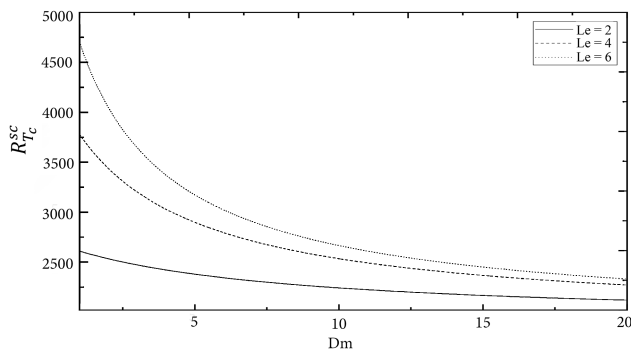


Figure 2. Change in the thermal critical Rayleigh number at the onset of stationary convection with the Damkohler number for distinct values of the Lewis number fixed at $R_S = 800$, $C_S = 0.04$ and $Ta = 50$.

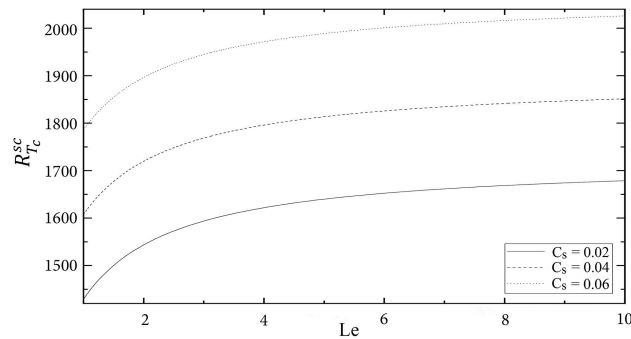


Figure 3. Change in the thermal critical Rayleigh number at the onset of stationary convection with the Lewis number for distinct values of the C_S parameter fixed at $R_S = 500$, $Dm = 25$ and $Ta = 50$.

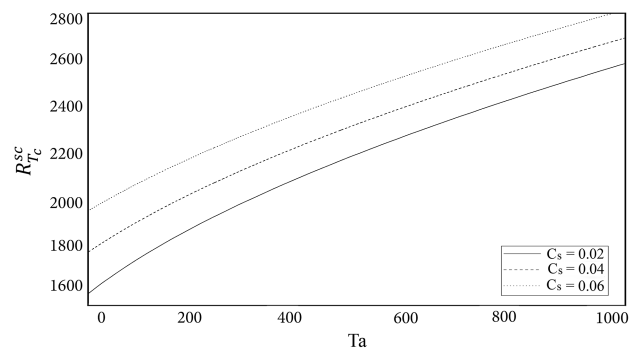


Figure 4. Change in thermal critical Rayleigh number at the onset of stationary convection with the Taylor number for distinct values of the C_S parameter fixed at $R_S = 500$, $Le = 5$ and $Dm = 25$.

Figure 4 illustrates that $R_{T_c}^{sc}$ with Ta for different values of C_S and for fixed at $R_S = 500$, $Le = 5$ and $Dm = 25$. In addition, it shows that, as C_S increases, $R_{T_c}^{sc}$ increases. As a result, it should be highlighted that a rise in C_S 's value stabilizes the system. An increase in the viscosity of a liquid, which slows down fluid motion, is represented by an increase in the values of C_S . As a result, the C_S parameter stabilizes convection.

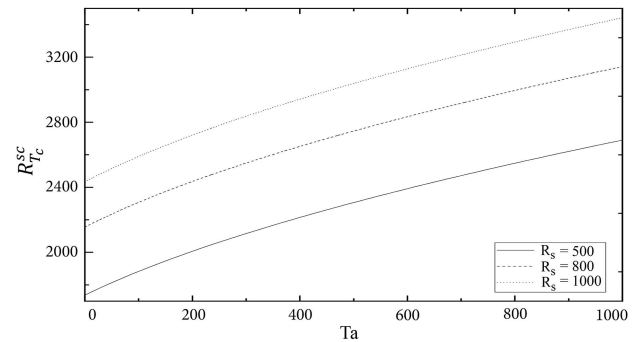


Figure 5. Change in the thermal critical Rayleigh number at the onset of stationary convection with the Taylor number for distinct values of the solute Rayleigh number fixed at $Dm = 25$, $C_S = 0.04$ and $Le = 5$.

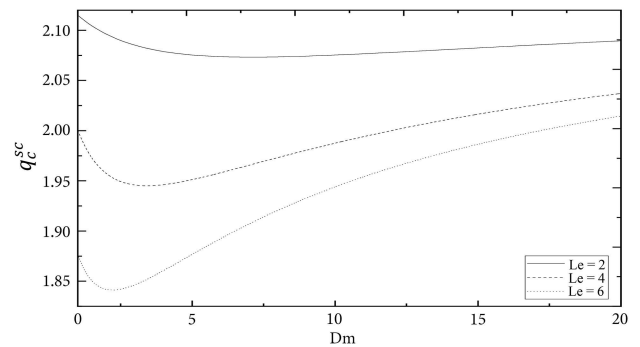


Figure 6. Change in the thermal critical wave number at the onset of stationary convection with the Damkohler number for distinct values of the Lewis number fixed at $R_S = 800$, $C_S = 0.04$ and $Ta = 50$.

The graph in Figure 5 illustrates the relationship between $R_{T_c}^{sc}$ and Ta , while holding distinct values of R_S constant at Dm, C_S, Le . It is evident from this graph that as the value of Ta increases, both $R_{T_c}^{sc}$ and R_S also increase, suggesting a positive correlation. This implies that Ta exerts a stabilizing influence on the system. The introduction of vorticity into the fluid as it rotates results in an accelerated flow in horizontal planes. However, this rotational motion causes a reduction in fluid velocity perpendicular to these planes. Consequently, there is an observed increase in $R_{T_c}^{sc}$ with the rise in Ta .

With varying values of Le , Figure 6 gives a visual representation of the critical wave number at the onset of stationary convection (q_c^{sc}) versus the Damkohler number (Dm). This figure makes it clear that, up to a certain point, the critical wave number decreases with an increasing value of $Dm = Dm^*$, and increases with Dm thereafter. Consequently, q_c^{sc} is a non-monotonic function of Dm .

Figure 7 illustrates the relationship between q_c^{sc} and Le for different values of C_S (0.02, 0.04, 0.06), with the remaining parameters held constant at $R_S = 500$, $Dm = 25$, $Ta = 50$. Within this figure, q_c^{sc} exhibits a decreasing trend as both Le and C_S increase, establishing q_c^{sc} as a decreasing function of Le and C_S . Furthermore, Figures 8 and 9 highlight the upward trajectory of q_c^{sc} concerning Ta , portraying its variation across different parameter values.

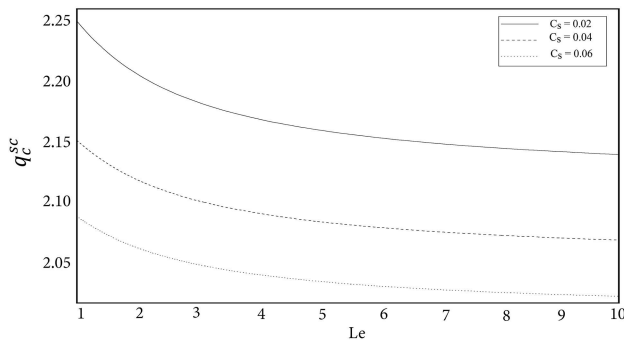


Figure 7. Change in the thermal critical wave number at the onset of stationary convection with the Lewis number for distinct values of the C_S parameter fixed at $R_S = 500$, $Dm = 25$ and $Ta = 50$.

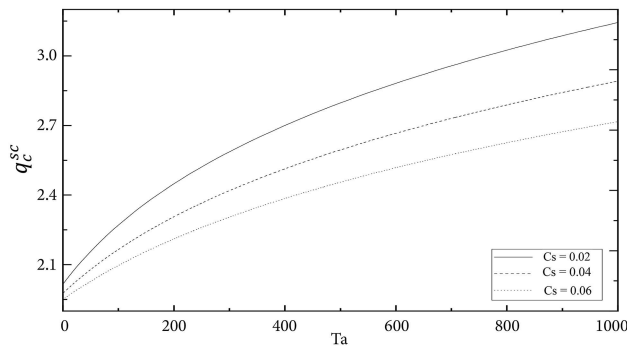


Figure 8. Change in the thermal critical wave number at the onset of stationary convection with the Taylor number for distinct values of the C_S parameter fixed at $R_S = 500$, $L_e = 5$ and $Dm = 25$.

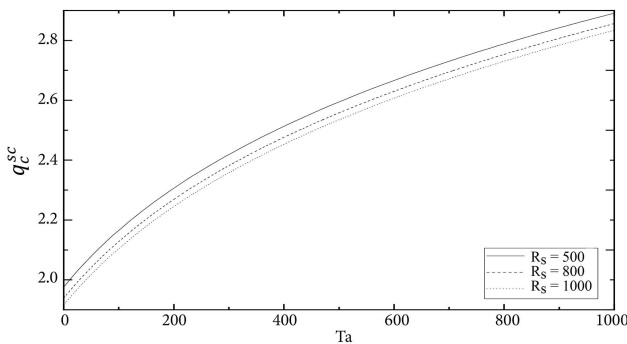


Figure 9. Change in the wave with the Taylor number for distinct values of the solute Rayleigh number fixed at $Dm = 25$, $C_S = 0.04$ and $L_e = 5$.

The behavior of the thermal critical Rayleigh number at the onset of oscillatory convection $R_{T_c}^{oc}$ versus Dm with different values of Le is depicted in Figure 10, the remaining parameters are held fixed. This figure unequivocally demonstrates that Dm increases as $R_{T_c}^{oc}$ decreases. Therefore, Dm has a destabilizing effect on the system. Figure 11 represents the variation of $R_{T_c}^{oc}$ versus Le for the different values of C_S fixed at $R_S = 500$, $Dm = 25$, $Ta = 50$ and $Pr = 0.0001$. This figure clearly shows the stabilizing effect of Le on the system. As the Lewis number decreases,

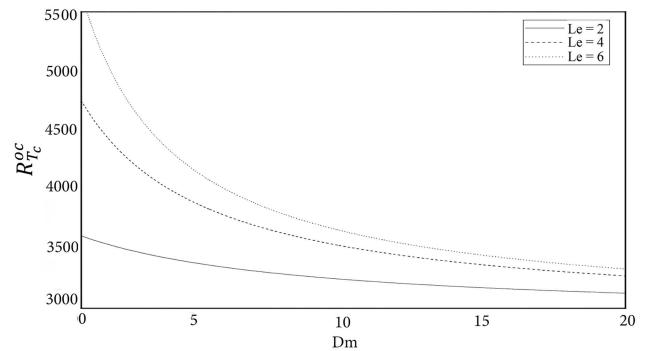


Figure 10. Change in the thermal critical Rayleigh number at the onset of oscillatory convection with the Damkohler number for distinct values of the Lewis number fixed at $R_S = 800$, $C_S = 0.04$, $Ta = 50$ and $Pr = 0.0001$.

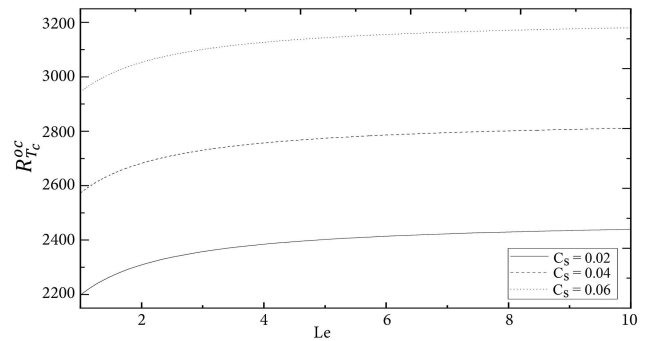


Figure 11. Change in the thermal critical Rayleigh number at the onset of oscillatory convection with the Lewis number for distinct values of the C_S parameter fixed at $R_S = 500$, $Dm = 25$, $Ta = 50$ and $Pr = 0.0001$.

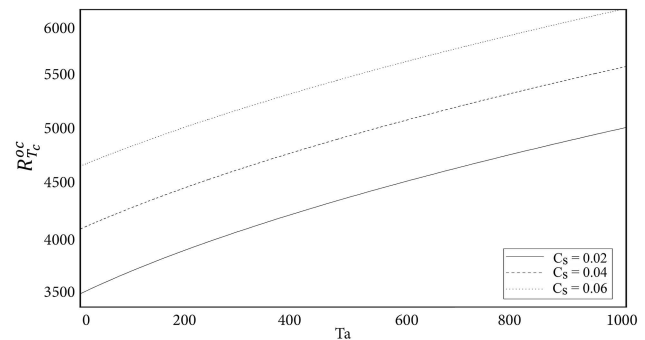


Figure 12. Change in the thermal critical Rayleigh number at the onset of oscillatory convection with the Taylor number for distinct values of the C_S parameter fixed at $R_S = 500$, $L_e = 5$, $Dm = 25$ and $Pr = 5$.

the distinction between solutal and thermal diffusivities diminishes, rendering it more challenging for inherently double diffusive processes, like the initiation of oscillatory convection, to transpire.

Figure 12 shows that $R_{T_c}^{oc}$ with Ta for distinct values of $C_S = 0.02, 0.04, 0.06$ and fixed values of R_S , Dm , Le and Pr . This figure shows that as C_S increases, $R_{T_c}^{oc}$ increases. Hence, Ta and C_S have a stabilizing effect on the system.

The behavior of $R_{T_c}^{oc}$ versus Ta with different values

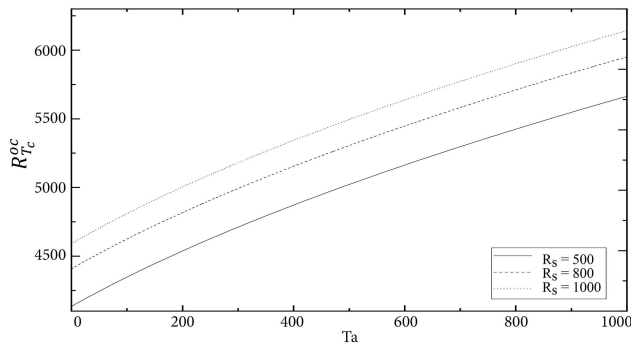


Figure 13. Change in the thermal critical Rayleigh number at the onset of oscillatory convection with the Taylor number for distinct values of the solute Rayleigh number fixed at $Dm = 25$, $C_S = 0.04$, $L_e = 5$ and $Pr = 5$.

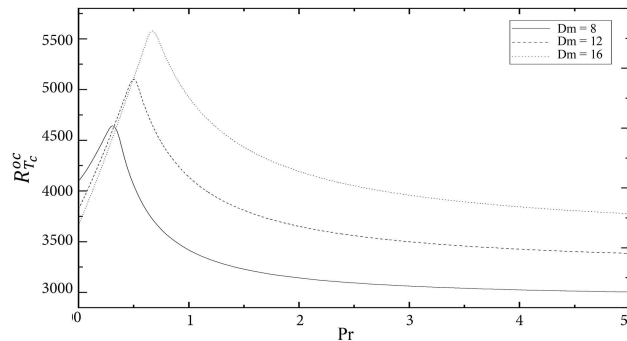


Figure 14. Change in the thermal critical Rayleigh number at the onset of oscillatory convection with the Prandtl number for distinct values of the Damkohler number when $R_S = 1000$, $C_S = 0.04$, $L_e = 5$ and $Ta = 50$.

of R_S is shown in Figure 13. All other parameters are held constant. The enhancement of $R_{T_c}^{oc}$ with the increase in the value of Ta is shown in this figure. It is noted that an increment in the value of Ta makes the system stable.

In Figure 14, $R_{T_c}^{oc}$ is plotted against the Prandtl number (Pr) for distinct values of $Dm = 8, 12, 16$ and for the fixed values of R_S , C_S , L_e and Ta . This figure shows that $R_{T_c}^{oc}$ increases with an increasing value of $Dm = Dm^*$, and beyond $Dm = Dm^*$, $R_{T_c}^{oc}$ decreases with Dm . Hence, $R_{T_c}^{oc}$ is a non-monotonic function of Pr .

Figure 15 depicts the critical wave number at the onset of oscillatory convection (q_c^{oc}) versus Dm for various values of L_e . This figure shows that Dm increases but q_c^{oc} decreases and then increases, indicating q_c^{oc} is a non-monotonic function of Dm .

Figure 16 depicts the linear instability thresholds with the q_c^{oc} versus L_e for different values of C_S , with the remaining parameters held constant at $R_S = 500$, $Dm = 25$, $Ta = 50$, and $Pr = 0.0001$. In this figure, q_c^{oc} decreases as L_e increases, but C_S decreases as q_c^{oc} increases.

Figure 17 represents q_c^{oc} versus Ta by taking into account distinct values of C_S at $R_S = 500$, $L_e = 5$, $Dm = 25$ and $Pr = 5$. The enhancement of q_c^{oc} with the enhancement in the value of Ta is observed. A similar trend of q_c^{oc} versus Ta can be observed in Figure 18.

We give some examples of steady or oscillatory insta-

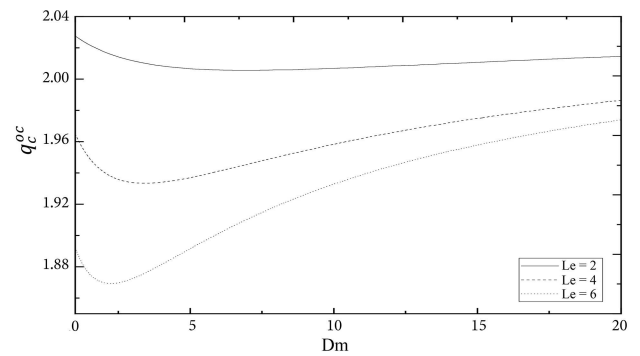


Figure 15. Change in the thermal critical wave number at the onset of oscillatory convection with the Damkohler number for distinct values of the Lewis number fixed at $R_S = 800$, $C_S = 0.04$, $Ta = 50$ and $Pr = 0.0001$.

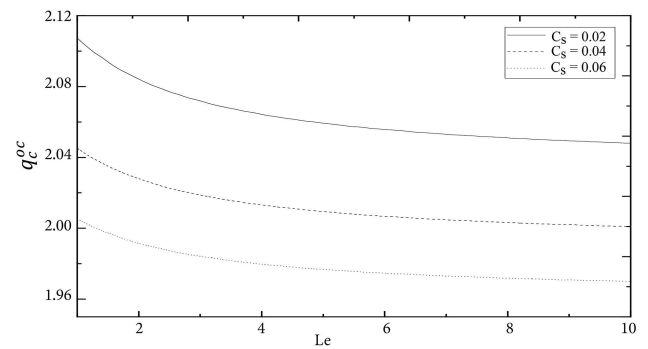


Figure 16. Change in the thermal critical wave number at the onset of oscillatory convection with the Lewis number for distinct values of the C_S parameter fixed at $R_S = 500$, $Dm = 25$, $Ta = 50$ and $Pr = 0.0001$.

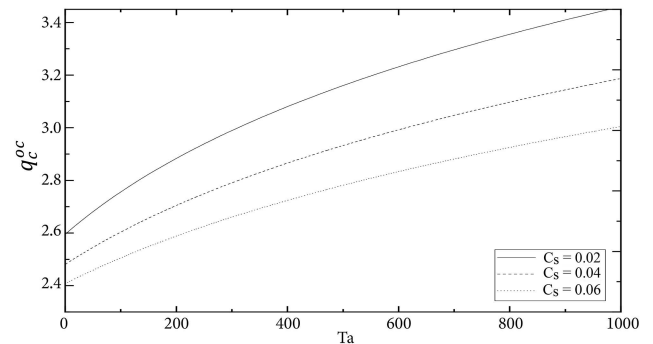


Figure 17. Change in the thermal critical wave number at the onset of oscillatory convection with the Taylor number for distinct values of the C_S parameter fixed at $R_S = 500$, $L_e = 5$, $Dm = 25$ and $Pr = 5$.

bility developing for constant values of physical parameters in Tables 1 and 2. According to Table 1, the stationary instability threshold occurs when $Ta \leq 910.331$, and convection is oscillatory when $Ta > 910.331$. From Table 2, we can see that the oscillatory instability threshold occurs when $Dm \leq 1.76455$, whereas the stationary convection dominates when $Dm > 1.76455$. To put it another way, oscillatory convection begins, but as soon as the value

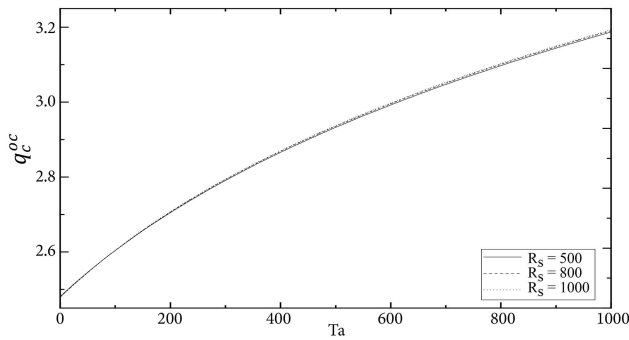


Figure 18. Change in the thermal critical wave number at the onset of oscillatory convection with the Taylor number for distinct values of the solute Rayleigh number fixed at $Dm = 25$, $C_S = 0.04$, $Le = 5$ and $Pr = 5$.

Table 1. Critical values of R_T for the case $Pr = 0.1$, $R_S = 800$, $Le = 5$, $Dm = 5$ and $C_S = 0.04$ (St. is for Stationary and Os. is for Oscillatory).

Ta	$R_{T_c}^{sc}$	q_c^{osc}	$R_{T_c}^{oc}$	q_c^{oc}	Instability
850	3953.117	2.672	4006.643	1.978	St.
860	3961.338	2.672	4005.879	1.978	St.
870	3969.509	2.682	4005.120	1.978	St.
880	3977.662	2.682	4004.364	1.978	St.
890	3985.747	2.691	4003.612	1.979	St.
900	3993.816	2.701	4002.865	1.979	St.
910	4001.834	2.702	4002.121	1.979	St.
910.331	4002.097	2.703	4002.097	1.979	St.
920	4009.822	2.710	4001.382	1.979	Os.
930	4017.775	2.714	4000.646	1.979	Os.
940	4025.683	2.720	3999.914	1.980	Os.
950	4033.571	2.726	3999.186	1.979	Os.

Table 2. Critical values of R_T for the case $Pr = 0.1$, $R_S = 800$, $Le = 5$, $Ta = 200$ and $C_S = 0.04$ (St. is for Stationary and Os. is for Oscillatory).

Dm	$R_{T_c}^{sc}$	q_c^{osc}	$R_{T_c}^{oc}$	q_c^{oc}	Instability
1	4489.224	2.177	3707.138	2.181	Os.
1.1	4429.914	2.169	3767.729	2.182	Os.
1.2	4373.429	2.162	3826.564	2.180	Os.
1.3	4319.584	2.156	3883.190	2.177	Os.
1.4	4268.209	2.150	3937.057	2.170	Os.
1.5	4219.144	2.146	3987.525	2.161	Os.
1.6	4172.243	2.142	4033.889	2.149	Os.
1.7	4127.372	2.138	4075.444	2.133	St.
1.76455	4099.427	2.137	4099.427	2.122	St.
1.8	4084.404	2.136	4111.601	2.115	St.
1.9	4043.223	2.133	4142.011	2.096	St.
2	4003.724	2.131	4166.667	2.077	St.

of Dm reaches a critical value (1.76455), it stops being oscillatory and the first bifurcation occurs as stationary convection.

5. Conclusion

In this article, we investigated the chemical reaction on the stability of thermo-solutal convection in a rotating C_S fluid. Various parameters such as R_T , q , R_S , Dm , Ta , Le , C_S and Pr have been studied. The following is a summary of the findings:

Stationary convection

- The Damkohler number has a destabilizing influence on a fluid layer;
- The Lewis, Taylor number and solute Rayleigh numbers have a stabilizing effect on the system;
- The critical wave number is a non-monotonic function of the Damkohler number;
- The critical wave number is a decreasing function of the Lewis number, solute Rayleigh number and C_S parameters;
- The critical wave number is an increasing function of the Taylor number.

Oscillatory convection

- As we saw in the case of stationary convection, the Damkohler number has a destabilizing effect on the fluid layer;
- The Lewis, Taylor and solute Rayleigh numbers have a stabilizing effect on the system;
- The critical Rayleigh number is a non-monotonic function of the Prandtl number;
- The critical wave number is a non-monotonic function of the Damkohler number;
- The critical wave number is a decreasing function of the Lewis number, solute Rayleigh number and C_S parameter;
- The critical wave number is an increasing function of the Taylor number.

Furthermore

- The stationary instability threshold occurs when $Ta \leq 910.331$ and convection is by oscillation when $Ta > 910.331$;
- The oscillatory instability threshold occurs when $Dm \leq 1.76455$, whereas the stationary convection dominates when $Dm > 1.76455$.

In future, we plan to explore the heat and mass transport by deriving the amplitude equation using weakly non-linear analysis. Also, we want to study the non-linear instability analysis using the energy method.

Nomenclature

P	Pressure
Pr	Prandtl number
R_T	Thermal Rayleigh number
R_S	Solutal Rayleigh number
β_T	Thermal expansion coefficient

β_S	Solutal expansion coefficient
ΔT	Temperature difference
t	Time
ΔS	Concentration difference
Dm	Damkohler number
q	Wave number
x, y, z	Coordinates
Ta	Taylor number
\mathbf{V}	Velocity
D_v	Solutal diffusivity
Ω	Angular velocity
T	Temperature
d	Height of fluid
g	Acceleration due to gravity
κ	Thermal diffusivity
μ	Dynamic viscosity
ρ	Density
μ_1	C_S viscosity
S	Concentration
Le	Lewis number
C_S	C_S parameter
ν	Kinematic viscosity

Superscripts

,	Perturbed quantity
---	--------------------

Subscripts

b	Basic state
c	Critical value
0	Reference value

Other symbols

$$\nabla^2 = \frac{\partial^2}{\partial x^2} + \frac{\partial^2}{\partial y^2} + \frac{\partial^2}{\partial z^2};$$

$$\nabla_h^2 = \frac{\partial^2}{\partial x^2} + \frac{\partial^2}{\partial y^2};$$

Acknowledgments

Funding

This research did not receive any specific grant from funding agencies in the public, commercial, or not-for-profit sectors.

Conflicts of interest

The authors declare that they have no known competing financial interests or personal relationships that could have appeared to influence the work reported in this paper.

Authors contribution statement

First author

Jangalla Nagaraju: Problem formulation; Solving; writing paper

Second author

Kasba Ramesh Babu: Editing

Third author

Gundlapally Shiva Kumar Reddy: Validation of results; Editing; Software

Fourth author

Kiran Kumar Paidipati: Editing; Software

Fifth author

Christophe Chesneau: Paper corrections; Editing; Technical writing

References

1. Gul, T., Nasir, S., Berrouk, A.S., et al. "Simulation of the water-based hybrid nanofluids flow through a porous cavity for the applications of the heat transfer", *Scientific Reports*, **13**(1), p. 7009 (2023). <https://doi.org/10.1038/s41598-023-33650-w>
2. Nasir, S., Berrouk, A.S., Aamir, A., et al. "Features of flow and heat transport of MoS₂+GO hybrid nanofluid with nonlinear chemical reaction, radiation and energy source around a whirling sphere", *Heliyon*, **9**(4), pp. 1-13 (2023). <https://doi.org/10.1016/j.heliyon.2023.e15089>
3. Nasir, S., Berrouk, A.S., Aamir, A., et al. "Entropy optimization and heat flux analysis of Maxwell nanofluid configured by an exponentially stretching surface with velocity slip", *Scientific Reports*, **13**(1), p. 2006 (2023). <https://doi.org/10.1038/s41598-023-29137-3>
4. Nasir, S., Berrouk, A.S., Aamir, A., et al. "Significance of chemical reactions and entropy on Darcy-forchheimer flow of H₂O and C₂H₆O₂ conveying magnetized nanoparticles". *International Journal of Thermofluids*, **17**, 100265 (2023). <https://doi.org/10.1016/j.ijft.2022.100265>
5. Nasir, S., Berrouk, A.S., Tassaddiq, A., et al. "Impact of entropy analysis and radiation on transportation of MHD advance nanofluid in porous surface using Darcy-Forchheimer model", *Chemical Physics Letters*, **811**, 140221 (2023). <https://doi.org/10.1016/j.cplett.2022.140221>
6. Nasir, S., Sirisubtawee, S., Juntharee, P., et al. "Heat transport study of ternary hybrid nanofluid flow under magnetic dipole together with nonlinear thermal radiation", *Applied Nanoscience*, **12**(9), pp. 2777-2788 (2022). <https://doi.org/10.1007/s13204-022-02583-7>
7. Alnahdi, A.S., Nasir, S., and Gul, T. "Ternary Casson hybrid nanofluids in convergent/divergent channel for the application of medication", *Thermal Science*, **27**(Spec. issue 1), pp. 67-76 (2023). <https://doi.org/10.2298/TSCI23S1067A>
8. Alnahdi, A.S., Nasir, S., and Gul, T. "Blood-based ternary hybrid nanofluid flow-through perforated capillary for the applications of drug delivery", *Waves*

- in *Random and Complex Media*, pp. 1-19 (2022). <https://doi.org/10.1080/17455030.2022.2134607>
9. Zeeshan, A., Hussain, F., Ellahi, R., et al. "A study of gravitational and magnetic effects on coupled stress bi-phase liquid suspended with crystal and Hafnium particles down in steep channel", *Journal of Molecular Liquids*, **286**, 110898 (2019). <https://doi.org/10.1016/j.molliq.2019.110898>
 10. Ellahi, R., Zeeshan, A., Hussain, F., et al. "Two-phase couette flow of couple stress fluid with temperature dependent viscosity thermally affected by magnetized moving surface", *Symmetry*, **11**(5), p. 647 (2019). <https://doi.org/10.3390/sym11050647>
 11. Bhatti, M.M., Zeeshan, A., Asif, M.A., et al. "Non-uniform pumping flow model for the couple stress particle-fluid under magnetic effects", *Chemical Engineering Communications*, **209**(8), pp. 1058–1069 (2022). <https://doi.org/10.1080/00986445.2021.1940156>
 12. Afzal, Q., Akram, S., Ellahi, R., et al. "Thermal and concentration convection in nanofluids for peristaltic flow of magneto couple stress fluid in a nonuniform channel", *Journal of Thermal Analysis and Calorimetry*, **144**, pp. 2203–2218 (2021). <https://doi.org/10.1007/s10973-020-10340-7>
 13. Khan, A.A., Bukhari, S.R., Marin, M., et al. "Effects of chemical reaction on third-grade MHD fluid flow under the influence of heat and mass transfer with variable reactive index", *Heat Transfer Research*, **50**(11), pp. 1-14 (2019). <https://doi.org/10.1615/HeatTransRes.2018028397>
 14. Ramesh, K., Mebarek-Oudina, F., Ismail, A.I., et al. "Computational analysis on radiative non-Newtonian Carreau nanofluid flow in a microchannel under the magnetic properties", *Scientia Iranica*, **30**(2), pp. 376–390 (2023). <https://doi.org/10.24200/sci.2022.58629.5822>
 15. Stokes, V.K. "Couple stresses in fluids", *Phys. Fluids*, **9**, pp. 1709–1715 (1966).
 16. Rubenstein, D.A. and Yin, W.M.D. "Frame Biofluid Mechanics", Academic Press, Wyman Street, Waltham, USA (2012).
 17. Singh, C. "Lubrication theory for couple stress fluids and its application to short bearings", *Wear*, **80**(3), pp. 281–290 (1982). [https://doi.org/10.1016/0043-1648\(82\)90256-3](https://doi.org/10.1016/0043-1648(82)90256-3)
 18. Srivastava, L.M. "Flow of couple stress fluid through stenotic blood vessels", *Journal of Biomechanics*, **18**(7), pp. 479–485 (1985). [https://doi.org/10.1016/0021-9290\(85\)90662-1](https://doi.org/10.1016/0021-9290(85)90662-1)
 19. Soundalgekar, V.M. and Chaturani, P. "Effects of couple-stresses on the dispersion of a soluble matter in a pipe flow of blood", *Rheologica Acta*, **19**(6), pp. 710–715 (1980). <https://doi.org/10.1007/BF01521862>
 20. Hsu, C.H., Lin, J.R., and Chiang, H.L. "Combined effects of couple-stresses and surface roughness on the lubrication of short journal bearings", *Ind. Lubr. Tribol.*, **55**, pp. 233–243 (2003). <https://doi.org/10.1108/00368790310488896>
 21. Sunil Devi, R. and Mahajan, A. "Global stability for thermal convection in a couple stress fluid", *Int. Commun. Heat Mass Transf.*, **38**, pp. 938–942 (2011). <https://doi.org/10.1016/j.icheatmasstransfer.2011.03.030>
 22. Shivakumara, I.S. "Onset of convection in a couple-stress fluid-saturated porous medium: effects of nonuniform temperature gradients", *Arch. Appl. Mech.*, **80**, pp. 949–957 (2010). <https://doi.org/10.1007/s00419-009-0347-5>
 23. Shivakumara, I.S., Sureshkumar, S., and Devaraju, N. "Coriolis effect on thermal convection in a couple-stress fluid-saturated rotating rigid porous layer", *Arch. Appl. Mech.*, **81**, pp. 513–530 (2011). <https://doi.org/10.1007/s00419-010-0425-8>
 24. Gaikwad, S.N. and Kouser, S. "Double diffusive convection in a couple stress fluid saturated porous layer with internal heat source", *Int. J. Heat Mass Transf.*, **78**, pp. 1254–1264 (2014). <https://doi.org/10.1016/j.ijheatmasstransfer.2014.07.021>
 25. Shivakumara, I.S. and Naveen Kumar, S.B. "Linear and non-linear triple diffusive convection in a couple stress fluid layer", *Int. J. Heat Mass Transf.*, **68**, pp. 542–553 (2014). <https://doi.org/10.1016/j.ijheatmasstransfer.2013.09.051>
 26. Srivastava, A.K. and Bera, P. "Influence of chemical reaction on stability of thermosolutal convection of couple-stress fluid in a horizontal porous layer", *Transp. Porous Media*, **97**(2), pp. 161–184 (2013). <https://doi.org/10.1007/s11242-012-0116-8>
 27. Malashetty, M.S. and Biradar, B.S. "The onset of double diffusive reaction- convection in an anisotropic porous layer", *Phys. Fluids*, **23**, 064102 (2011). <https://doi.org/10.1063/1.3598469>
 28. Ravi, R., Kanchana, C., and Siddheshwar, P.G. "Effects of second diffusing component and cross diffusion on primary and secondary thermoconvective instabilities in couple stress liquids", *Appl. Math. Mech. -Engl. Ed.*, **38**(11), pp. 1579–1600 (2017). <https://doi.org/10.1007/s10483-017-2280-9>
 29. Wollkind, D.J. and Frisch, H.L. "Chemical instabilities: I. A heated horizontal layer of dissociating fluid", *The Physics of Fluids*, **14**(1), pp. 13–18 (1971). <https://doi.org/10.1063/1.1693263>
 30. Wollkind, D.J. and Frisch, H.L. "Chemical instabilities. III. Nonlinear stability analysis of a heated horizontal layer of dissociating fluid", *The Physics of Fluids*, **14**(3), pp. 482–487 (1971). <https://doi.org/10.1063/1.1693460>
 31. Bdzil, John B. and Frisch, H.L. "Chemically driven convection", *The Journal of Chemical Physics*, **72**(3), pp. 1875–1886 (1980). <https://doi.org/10.1063/1.439332>

32. Steinberg, V. and Brand, H. "Convective instabilities of binary mixtures with fast chemical reaction in a porous medium", *The Journal of Chemical Physics*, **78**(5), pp. 2655–2660 (1983). <https://doi.org/10.1063/1.445024>
33. Steinberg, V. and Brand, H.R. "Amplitude equations for the onset of convection in a reactive mixture in a porous medium", *The Journal of Chemical Physics*, **80**(1), pp. 431–435 (1984). <https://doi.org/10.1063/1.446466>
34. Gatica, J.E., Viljoen, H.J., and Hlavacek, V. "Interaction between chemical reaction and natural convection in porous media", *Chemical Engineering Science*, **44**(9), pp. 1853–1870 (1989). [https://doi.org/10.1016/0009-2509\(89\)85127-9](https://doi.org/10.1016/0009-2509(89)85127-9)
35. Pritchard, D. and Richardson, C.N. "The effect of temperature-dependent solubility on the onset of thermosolutal convection in a horizontal porous layer", *Journal of Fluid Mechanics*, **571**, pp. 59–95 (2007). <https://doi.org/10.1017/S0022112006003211>
36. Wang, S. and Tan, W. "The onset of Darcy-Brinkman thermosolutal convection in a horizontal porous media", *Physics Letters A*, **373**(7), pp. 776–780 (2009). <https://doi.org/10.1016/j.physleta.2008.12.056>
37. Hill, A.A. and Morad, M.R. "Convective stability of carbon sequestration in anisotropic porous media". *Proceedings of the Royal Society A: Mathematical, Physical and Engineering Sciences*, **470**(2170), 20140373 (2014). <https://doi.org/10.1098/rspa.2014.0373>
38. Ward, T.J., Cliffe, K.A., Jensen, O.E. et al. "Dissolution-driven porous-medium convection in the presence of chemical reaction", *Journal of Fluid Mechanics*, **747**(20T), pp. 316–349 (2014). <https://doi.org/10.1017/jfm.2014.149>
39. Sulaimi, A.B. "The energy stability of Darcy thermosolutal convection with reaction", *International Journal of Heat and Mass Transfer*, **86**, pp. 369–376 (2015). <https://doi.org/10.1016/j.ijheatmasstransfer.2015.03.007>
40. Gautam, K. and Narayana, P.A.L. "On the stability of carbon sequestration in an anisotropic horizontal porous layer with a first-order chemical reaction", *Proceedings of the Royal Society A*, **475**(2226), 20180365 (2019). <https://doi.org/10.1098/rspa.2018.0365>
41. Reddy, G.S.K. and Ragoju, R. "Thermal instability of a Maxwell fluid saturated porous layer with chemical reaction", *Spec. Top. Rev. Porous Media Int. J.*, **13**, pp. 33–47 (2022). <https://doi.org/10.1615/SpecialTopicsRevPorousMedia.2021037410>
42. Reddy, G.S.K., Koteswararao, N.V., Ravi, R., et al. "Dissolution-driven convection in a porous medium due to vertical axis of rotation and magnetic field", *Mathematical and Computational Applications*, **27**(3), p. 53 (2022). <https://doi.org/10.3390/mca27030053>
43. Ahlers, G., Grossmann, S., and Lohse, D. "Heat transfer and large scale dynamics in turbulent Rayleigh-Benard convection", *Rev. Modern Phys.*, **81**, p. 503 (2009). <https://doi.org/10.1103/RevModPhys.81.503>
44. Lohse, D. and Xia, K.Q. "Small-scale properties of turbulent Rayleigh-Benard convection", *Annu. Rev. Fluid Mech.*, **42**, pp. 335–364 (2010). <https://doi.org/10.1146/annurev.fluid.010908.165152>
45. Hassler, D., Dammasch, I., Lemaire, P., et al. "Solar wind outflow and the chromospheric magnetic network", *Science*, **283**(5403), pp. 810–813 (1999). <https://doi.org/10.1126/science.283.5403.810>
46. Johnston, J.P. "Effects of system rotation on turbulence structures: a review relevant to turbomachinery flows", *Int. J. Rot. Mach.*, **4**(2), pp. 97–112 (1998). <https://doi.org/10.1155/S1023621X98000098>
47. Hartmann, D.L., Moy, L.A., and Fu, Q. "Tropical convection and the energy balance at the top of the atmosphere", *J. Clim.*, **14**, pp. 4495–4511 (2001). [https://doi.org/10.1175/1520-0442\(2001\)014<4495:TCATEB>2.0.CO;2](https://doi.org/10.1175/1520-0442(2001)014<4495:TCATEB>2.0.CO;2)
48. Marshall, J. and Schott, F. "Open-ocean convection: observations, theory, and models", *Rev. Geophys.*, **37**, pp. 1–64 (1999). <https://doi.org/10.1029/98RG02739>
49. Babu, A.B., Reddy, G.S.K., and Tagare, S.G. "Nonlinear magneto convection due to horizontal magnetic field and vertical axis of rotation due to thermal and compositional buoyancy", *Results in Physics*, **12**, pp. 2078–2090 (2019). <https://doi.org/10.1016/j.rinp.2019.02.022>
50. Benerji Babu, A., Reddy, G.S.K., and Tagare, S.G. "Nonlinear magnetoconvection in a rotating fluid due to thermal and compositional buoyancy with anisotropic diffusivities", *Heat Transfer-Asian Research*, **49**(1), pp. 335–355 (2020). <https://doi.org/10.1002/htj.21615>
51. Rahmstorf, S. "The thermohaline ocean circulation: a system with dangerous thresholds?" *Clim. Change*, **46**, pp. 247–256 (2000). <https://publications.pik-potsdam.de/pubman/item/item-11819>
52. Chandrasekhar, S. "Hydrodynamic and hydromagnetic stability", Courier Corporation (2013).

Biographies

Jangalla Nagaraju completed his MSc in mathematics at Osmania University in 2013. He qualified for the CSIR-UGCNET. In the year 2016, he is pursuing his PhD at Osmania University under the supervision of Dr. Ramesh Babu in the area of applied mathematics and fluid dynamics. He has published two research papers, and he has two years of teaching experience in various engineering colleges.

Kasba Ramesh Babu is currently working as an Assistant Professor in mathematics at the University College of Engineering, Osmania University, India. His research areas are applied mathematics, fluid dynamics, and boundary

layer theory. He has published several articles in reputed international journals.

Gundlapally Shiva Kumar Reddy is working as an Assistant Professor in the Department of Applied Sciences, National Institute of Technology Goa, Goa, India. He has published more than 15 articles in various reputed journals. He received his PhD from the National Institute of Technology, Warangal, Telangana, India. His research interests include hydrodynamic stability, convection in porous media, linear and non-linear stability analyses, and artificial neural networks.

Kiran Kumar Paidipati is working as an Assistant Professor in the area of decision sciences at the Indian Institute of Management, Sirmaur, Himachal Pradesh,

India. Paidipati completed his PhD in statistics and post-doctoral studies from Pondicherry University, Puducherry, India, and his MSc in statistics from Sri Venkateswara University, Tirupati, India. His research areas include stochastic modeling, operations research, and data science. He has published more than 25 research papers in various reputed journals.

Christophe Chesneau got his PhD from the University of Paris in 2006. He's been a Teacher and Researcher at Université de Caen-Normandie, France, since 2007. He is actually an assistant professor with the “habilitation à diriger les recherches”. With extensive expertise in a wide area of applied science, Christophe Chesneau has made significant contributions to more than three hundred international publications.